

5th CIRP CSI 2020

Milling parameter and tool wear dependent surface quality in micro-milling of brass

Stephan Dehen^{a,*}, Eric Segebade^a, Michael Gerstenmeyer^a, Frederik Zanger^a, Volker Schulze^a

^a*wbk Institute of Production Science, Karlsruhe Institute of Technology (KIT), Kaiserstr. 12, 76131 Karlsruhe, Germany*

* Corresponding author. Tel.: +49-721-608-42455; fax: +49-721-608-45004; E-mail address: stephan.dehen@kit.edu

Abstract

Short life-time and high tool costs still remain major constraints for the micro-milling process. Understanding the wear mechanisms and their effects on the workpiece quality is essential for efficient tool usage. Usually, wear increases the cutting forces and reduces the emerging surface quality during the micro-milling process. Due to high tool costs, cutting parameters are usually chosen for optimal tool lifetime and/or process time rather than optimal surface quality.

The scope of this paper is to investigate the correlation of the process parameters, strategy and wear status of the tool on the resulting surface topography. To reach this goal, micro-milling experiments were conducted, in which several grooves were milled using two end milling tools, new and worn, with a diameter of 1.5 mm and four cutting edges. The cutting speed and feed were varied, as well as the cutting direction. Brass was chosen as workpiece material to ensure a constant wear state of the tools during the experiments. During the cutting process the process forces were recorded and examined for their magnitude and frequency response. Furthermore, the grooves were analyzed optically for their surface roughness.

The roughness shows in most cases slightly higher values for the specimen manufactured with the worn tool than the ones done with the new tool. The biggest influence on the surface roughness results from the feed rate, while cutting speed and milling strategy have a smaller influence. The measured cutting forces show similar tendencies, than the resulting surface roughness. The results show also a significant influence of tool wear on the vibration behavior during the process, while the influence of feed rate is mostly negligible. This results partly from the greater tool runout and bigger deviation of the cutting edges.

© 2020 The Authors. Published by Elsevier B.V.

This is an open access article under the CC BY-NC-ND license (<http://creativecommons.org/licenses/by-nc-nd/4.0/>)

Peer-review under responsibility of the scientific committee of the 5th CIRP CSI 2020

Keywords: micro milling; roughness; wear

1. Introduction

For over more than 5'000 years, copper and its alloys played an important role in the economic and social development of mankind [1] and by 2014 had reached a historic maximum consumption of 27 million tonnes worldwide. Copper, which is mainly used because of its high electrical and thermal conductivity, shows further positive aspects in combination with alloying elements (e.g. Zn, Sn or Pb) such as good machinability, bactericidal effect and high corrosion resistance. One of the most important copper alloys is brass, a combination

of copper and zinc that has higher strength and hardness than pure copper.

The micro-milling process is defined as a cutting process with geometrical defined cutting edges and tool diameters ranging from around (1-999 μm) [2]. It has established itself in the micro machining scene due to its superior removal rate, higher precision and flexibility compared to other micro production processes [3]. Micro-milling also has some disadvantages. While the cutting depth a_p in normal cutting processes is usually greater than the cutting radius r_β and the material can be assumed to be homogeneous, these cutting mechanisms change in micro-milling. Due to an extremely small ratio of

cutting radius to chip thickness, various effects such as chip thickness effect [4], ploughing [5] and other size effects [6] gain in importance, leading to increased tool wear and shortened tool life.

The most common types of wear in micro-milling are of abrasive or adhesive nature. Often, material adhesion on the cutting edge leads to increased cutting forces and thus to higher wear. This can occur on the flanks, surfaces or outer edges of the tool [7]. In addition, it is not easy to track tool behavior to a critical state of wear, as micro milling tools often break prematurely due to their fragile structure [8].

Since the workpiece-tool interaction in micro-milling is a rather complex mixture of cutting, rubbing and burnishing depending on the current geometry of the tool and is subject to abrupt changes due to wear, it is almost impossible to predict the resulting surface roughness [7]. According to Oliaei and Karpat [9] the resulting surface roughness R_a and R_z correlates with the wear volume of the tool during micro-milling of AISI 420.

So far, many studies have been carried out to investigate the influence of different process parameters and tool geometries on the wear behavior of the tool. It has been shown that tool wear in micro-milling behaves similarly to macro-milling when the cutting speed v_c is increased [8]. The feed f_z also has a large influence on the process result. If the correct choice is made, a constant chip behavior is triggered, which leads to lower cutting force fluctuations and thus to a more uniform surface quality [10]. If the feed per tooth f_z is too small, it may happen that not every tooth produces a chip, but only rubs against the surface [11]. Aurich et al. [12] investigated the influence of the spindle tilt angle on the resulting surface and chip formation. He showed that a small tilt angle leads to a surface with low roughness and smaller shape deviations. The influence of cutting parameters on the micro-milling of CuZn39Pb was analyzed by Tamborlin et al. [13]. They showed that the main influence on the resulting surface roughness is caused by the feed per tooth, while the cutting depth and overlap only have a small affect. They did not detect the occurrence of ploughing effects, since their minimal feed was above the radius of the peripheral cutting edge. An investigation of cutting parameters on wear and cutting forces during the micro-milling of pure copper was performed by Rahman et al. [14] in 2001. They discovered, that wear behavior was mostly of abrasive nature on the tool corner radii. The wear was non-uniform, therefore leading to great unbalance and premature tool breakage.

However, nearly no investigations were carried out on the influence of different cutting parameters and wear conditions on the resulting surface quality. Especially with very ductile materials, such as copper and its alloys, the choice of ideal cutting parameters can lead to an optimized cutting behavior by reducing the material adhesion on the cutting edges, reducing the unbalance of the tool and increasing the surface quality.

This paper analyses the influence of cutting parameters, milling strategy and tool wear on the resulting surface roughness.

Nomenclature

D	tool diameter
z	number of cutting edges
v_c	cutting speed
a_e	radial overlap
a_p	cutting depth
f_z	feed per tooth
F_c	cutting force
F_p	passive force

Experimental setup

The experiments were carried out with a five-axis high-precision micro-milling machine tool *KERN Pyramid Nano* from *KERN Microtechnik GmbH*. It has hydrostatic axes with a position accuracy of $1 \mu\text{m}$, a maximum acceleration above 1g and a maximum spindle speed of $50'000 \text{ min}^{-1}$. The tools were clamped with the *Tribos* clamping system of *Schunk GmbH & Co. KG*, with a dynamic rotational accuracy below $3 \mu\text{m}$. For the tests, two end mills with four cutting edges and a diameter of $D = 1.5 \text{ mm}$ were used. The tools were made of cemented carbide without coating. One tool was new, while the other was already in a worn condition (see section 2.1). Both tools were analyzed with the confocal light microscope *Infinite Focus* from *Alicona Imaging GmbH*.

A series of face milling experiments in the copper alloy CuZn39Pb3 with the new and worn tool was performed. The correspondent setup is illustrated in Fig. 1.

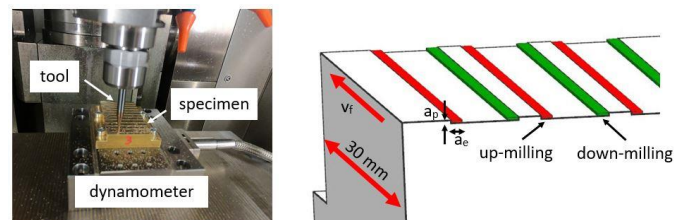


Fig. 1. Setup of the conducted experiments

The material was chosen, due to its good machinability, which ensures a constant state of tool wear during the experiments. Cutting speed, feed per tooth and the rotation direction were varied full factorial, while the cutting depth and the overlap remained constant. The selected parameters are shown in Table 1. All experiments were performed three times.

Table 1. Cutting parameters for the experiments.

Cutting parameters	Value
Cutting speed v_c	25, 50, 75, 100 m/min
Feed per tooth f_z	5, 10, 15 μm
Rotation direction	Up-/down-milling
Cutting depth a_p	50 μm
Overlap a_e	375 μm

During milling, the passive and active forces were measured with a three-axis dynamometer from *Kistler Instrumente AG*. It has a maximum measuring range of ± 250 N, a threshold value of 0.002 N and a natural frequency of 5.5 kHz. Due to the high measuring rate of 3333 Hz, it is possible to perform a Short-Time-Fourier transform to analyze the cutting force for its frequency composition. This enables the measuring of cutting edges in contact per revolution. Due to the limited measuring rate, however, only the measurements for a cutting speed of $v_c = 50$ m/min could be analyzed.

The resulting surfaces and their roughness were scanned with a confocal light microscope μ Surf from *NanoFocus AG* with a magnification of up to 100x, a lateral resolution of 0.2 μ m and a vertical resolution of 1 nm.

2. Results and Discussion

2.1. Tool measurements

The 3D confocal light microscopic measurements of the end mills are displayed in Fig. 2 and Table 2.

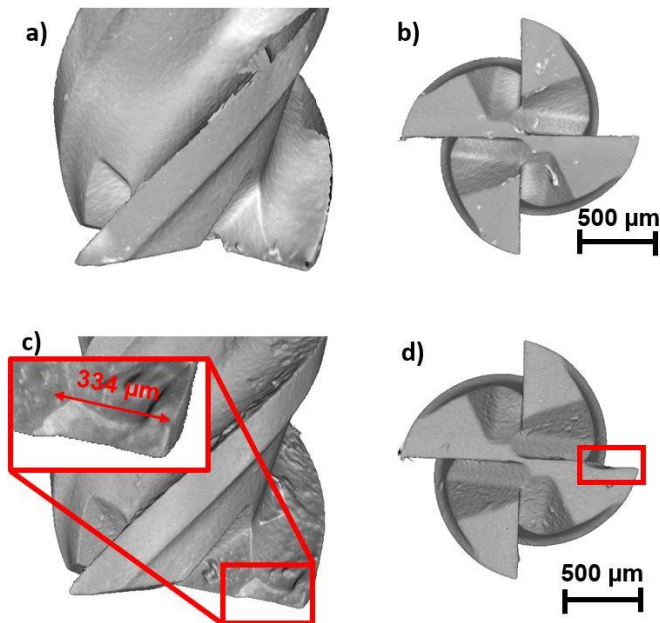


Fig. 2. Display of measured micro-milling new (a-b) and worn (c-d) micro-milling tool.

Table 2. Measured dimensions of the micro-milling tools

Dimension	New tool	Worn tool
Tool diameter D / μ m	1482.7	1475.1
Radius of peripheral cutting edge / μ m	13.88 ± 1.01	15.12 ± 2.10
Radius of end cutting edge / μ m	12.56 ± 0.48	16.90 ± 2.41

The new tool (a-b) shows a clear rake face and intact cutting edge, while the worn tool (c-d) exhibits combined face and outside edge wear (marked red), as well as material adhesion on the rake face. According to the measured data, the tool diameter of the worn tool is 7.6 μ m smaller than from the new tool. The average radius of the peripheral cutting edge, as well as of the end cutting edge is large for the worn tool, as for the

new tool. In both cases the standard deviation is larger for the worn tool. This indicates non-uniform abrasive face and outer edge wear too.

The tool runout, shown in Fig. 3, shows a larger value and deviation for the worn tool, than for the new tool, which could introduce a larger unbalance and therefore a worse vibration behaviour.

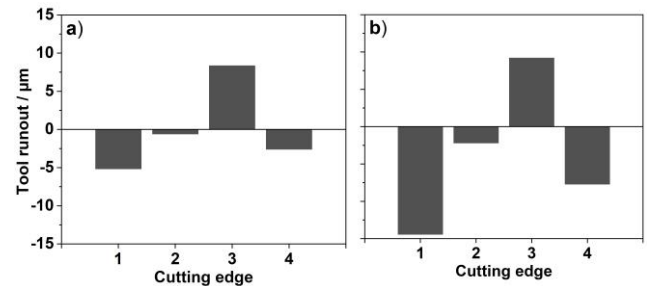


Fig. 3. Measured tool runout for the new (a) and worn (b) tool.

2.2. Cutting forces

The measured cutting forces of the experiments are shown in Fig. 4. As can be seen, the cutting forces of the worn tool (b) during the down-milling process are higher than those of the new tool (a). This could be explained by the locally larger cutting edge due to wear, which leads to a local negative rake angle and thus to ploughing effects and higher cutting forces.

For both tools, the average cutting forces increase with the feed per tooth, while for the new tool the cutting speed has almost no effect and a low reduction effect for the worn tool. A higher feed per tooth leads to a greater chip cross section and thus to higher cutting forces. When milling upwards, the cutting forces of the worn tool (d) are also higher than for the new tool (c). In addition, the cutting forces increase with rising feed rate during up-milling. They also grow with the cutting speed for the new tool, while remaining constant for the worn tool. The standard deviations of the cutting force for both

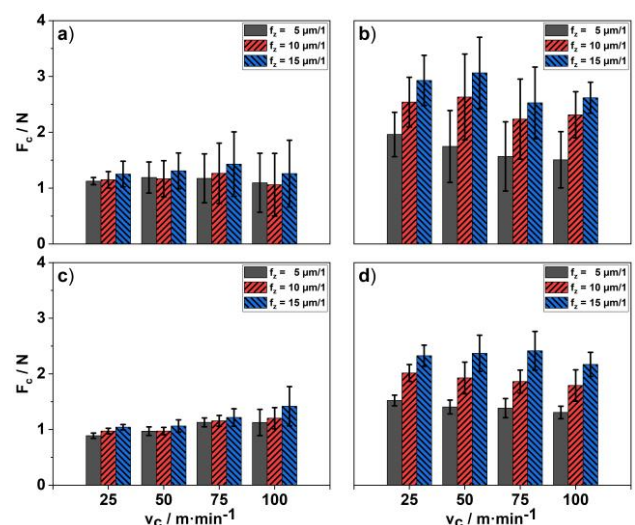


Fig. 4. Display of the cutting forces, measured during the experiments. First row: down-milling with the new (a) and worn (b) tool. Second row: up-milling with the new (c) and worn (d) tool.

milling strategies is larger for the worn tool, than for the new tool. This can be explained by the influence of the larger tool runout of the worn tool and therefore higher vibrations, resulting in fluctuations in the cutting forces.

2.3. Passive forces

The observed passive forces of the experiments are illustrated in Fig. 5. It is clearly visible that during down-milling the passive forces for the new tool (a) are higher than for the worn tool (b). This is exactly the opposite of what is expected. Normally the enlarged radius of the end cutting edge (see Table 2) would lead to a higher negative rake angle and

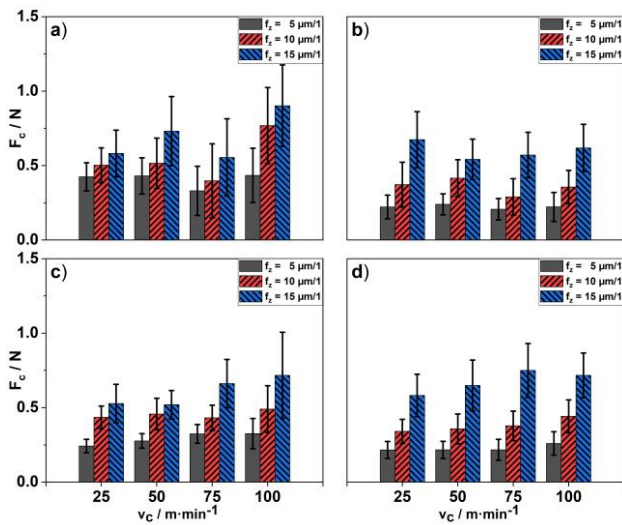


Fig. 5. Display of the passive forces, measured during the experiments. First row: down-milling with the new (a) and worn (b) tool. Second row: up-milling with the new (c) and worn (d) tool.

thus to ploughing and higher passive forces. The passive force also increases with the cutting speed and the feed rate for the new tool, while it only increases with the feed rate for the worn tool and remains constant when the cutting speed is risen. During the up-milling strategy, the passive forces grow with the feed rate, but remain the same when the cutting speed is increased. In addition, the passive forces for the new tool (c) and the worn tool (d) are very similar. It can be noted that the standard deviation of the passive forces of the up- and down-milling are very much alike. This is not consistent with the evaluation of the cutting forces. An explanation for this could be that the sample was mounted on the dynamometer and the x- and y-directions are in the mounting plane. By nature this setup is stiffer in axial than transversal direction, resulting in lower axial vibration.

2.4. Frequency analysis

The measured cutting forces were evaluated for its frequency response, using the short time fourier transformation (STFT). For a sampling rate of 3333 Hz, a Gaussian window with size 1024 and an overlap of 922 was applied. Due to the limited sampling rate, only the experiments with $v_c = 50 m/min$, were investigated. The STFT for the new tool, down-milling

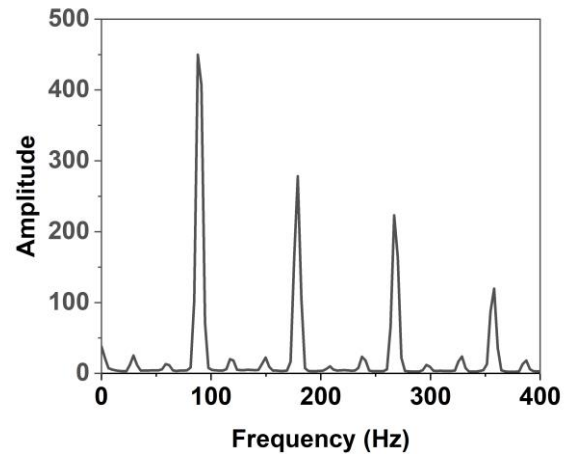


Fig. 6. Display of frequency response of the cutting force signal for the new tool, $f_z = 5 \mu m$ and $v_c = 50 m/min$.

strategy and $f_z = 5 \mu m$ is illustrated in Fig. 6. In the plot four significant peaks can be observed. The first is located at 88 Hz, the second at 177 Hz, the third at 265 Hz and the fourth at 354 Hz. With a spindle speed of $5305 min^{-1}$ and $z = 4$, the fourth peak represents the impact frequency of the cutting edges (IPF):

$$IPF = \frac{n \cdot z}{60} (Hz)$$

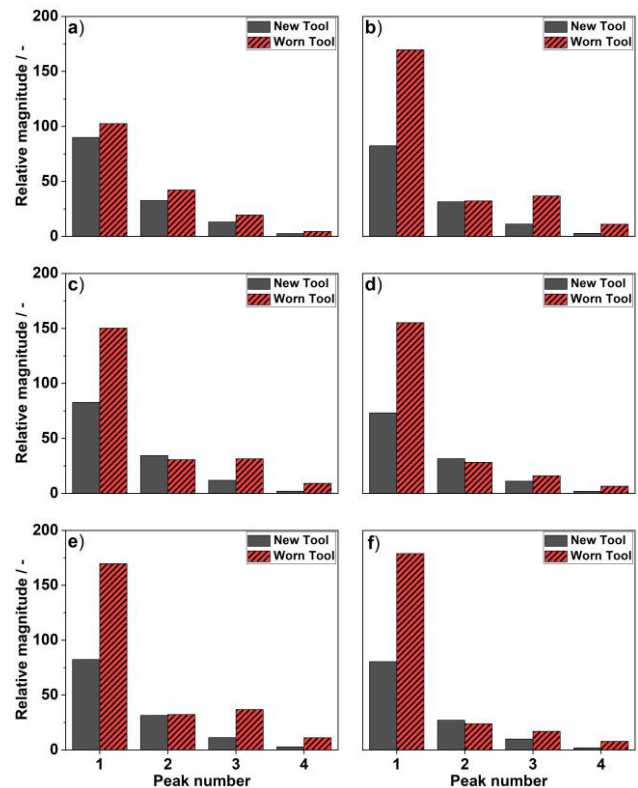


Fig. 7. Display of evaluated peak magnitude of the frequency response of the cutting force, measured during the experiments. First row: down- (a) and up- (b) milling for $f_z = 5 \mu m$. Second row: down- (c) and up- (d) milling for $f_z = 10 \mu m$. Third row: down- (e) and up- (f) milling for $f_z = 15 \mu m$.

While the first peak represents the dominant frequency rising from the spindle feed.

In the following analysis the relative magnitude for the fourth different peaks is evaluated and compared in Fig. 7. It demonstrates that for all feed rates, the relative magnitude of vibrations is larger for the worn tool than for the new one. That can be caused by the larger cutting edge radii, non-uniform tool wear and larger tool runout (see section 2.1). Also the most dominant frequency peak is number one, caused by the spindle rotation frequency.

The results show also that for $f_z = 5 \mu\text{m}$ and the new tool produces similar vibrations for down- (a) and up- (b) milling, while the worn tool exhibits a larger deviation in the relative magnitude.

With $f_z = 10 \mu\text{m}$ and $f_z = 15 \mu\text{m}$, the results look very similar (c - f). The worn tool shows the highest vibration for the first peak, which means for the spindle speed frequency. That could be explained by the huge non-uniform tool-runout and unstable tool-workpiece interactions.

2.5. Surface roughness

The surface was analyzed on an area of $160 \times 1600 \mu\text{m}$ using a confocal light microscope. To extract the surface roughness parameters, a SL-filter with a cut-off length of $\lambda_c = 0.25 \text{ mm}$. The resulting surface roughness parameters are given in Fig. 8. When down-milling (a - b), the surface roughness increases with the feed per tooth (except at $v_c = 75 \text{ m/min}$), while the influence of the cutting speed can be neglected. In general, the new tool tends to produce a better surface quality than the worn tool which was to be expected. Certain results with the new tool, feed $f_z = 15 \mu\text{m}$ and cutting speed $v_c = 25/50 \text{ m/min}$, show large standard deviations in surface roughness along one of the grooves. In both cases, the surface topography (pictured in Fig. 9) shows a damaged surface, which could be due to the poor chip removal without cooling fluid or air. Cooling was not

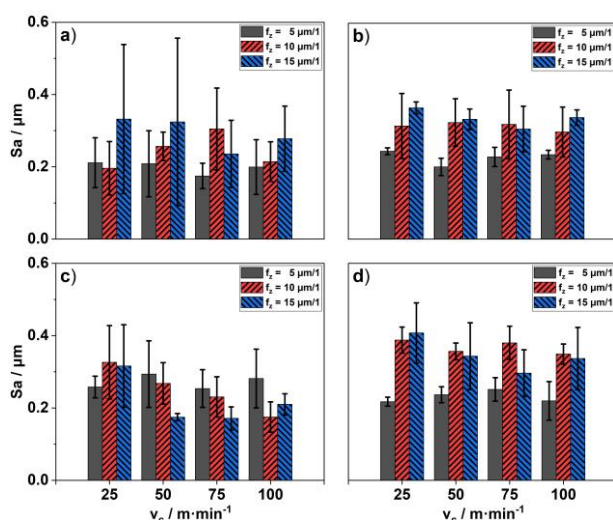


Fig. 8. Display of the resulting surface roughness S_a , measured after the experiments. First row: down-milling with the new (a) and worn (b) tool. Second row: up-milling with the new (c) and worn (d) tool.

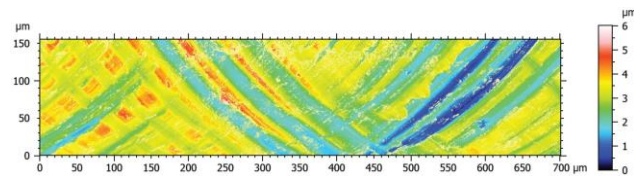


Fig. 9. Measured surface of the $v_c = 25 \text{ m/min}$, $f_z = 15 \mu\text{m}$, down-milling, new tool - sample

performed during the experiments, since the pressure would influence the cutting force measurements.

During the up-milling (c - d) the tendencies differ strongly from the downward milling experiments. With the new tool, the surface quality tends to improve with increasing cutting speed. At higher cutting speeds (50 and 100 m/min) the surface roughness decreases with rising feed rate. When using the worn tool, the surface quality is generally worse than with the new tool, except at a low feed rate of $f_z = 5 \mu\text{m}$, with the worn tool giving better results than the new tool.

3. Conclusion

The present paper deals the analysis of the influence of cutting parameters, machining strategy and tool wear on the surface roughness.

For this, micro-end milling experiments were conducted in brass, with varying cutting parameters, milling strategies and different tool wear states. The process forces were measured in-process, while the resulting surface roughness was measured afterwards. The forces were analyzed on their magnitude as well as for their frequency composition, indicating how often they cut per revolution.

The results reveal that the tool wear and the feed rate generally increase the cutting forces, while the cutting speed tends to decrease the cutting forces. The surface quality behaves instable, which means that no real tendencies could be detected. The general assumption, that high tool wear creates a worse surface quality could not be verified. The instable behavior was also detected by analyzing the frequency behavior of the cutting forces.

Acknowledgements

The authors thank the DFG, the Deutsche Forschungsgemeinschaft (German Research Foundation) for support of the investigations within the funding INST 121384/59.

References

- [1] <https://copperalliance.org.uk/copper-industry/copper-market/>, Accessed: 08.12.2019.
- [2] Mativenga P. (2019) Micromachining. In: Chatti S., Laperrière L., Reinhart G., Tolio T. (eds) CIRP Encyclopedia of Production Engineering. Springer, Berlin, Heidelberg.
- [3] Davim JP. Modern Mechanical Engineering. Springer. Berlin. 2014.
- [4] De Oliveira FB, Rodrigues AR, Coelho RT, de Souza AF. Size effect and minimum chip thickness in micromilling. Int. J. Mach. Tools Manuf. 2015; 89:39-54.

- [5] Wan M, Ma YC, Feng J, Zhang WH. Study of static and dynamic ploughing mechanisms by establishing generalized model with static milling forces. *Int. J. Mech. Sci.* 2016; 114:120-131.
- [6] Zhang J, Shuai M, Zheng H, Li Y, Jin M, Sun T. Atomistic and Experimental Investigation of the Effect of Depth of Cut on Diamond Cutting of Cerium. *Micromachines.* 2018; 9:26.
- [7] Alhaldeff LL, Marhall MB, Curtis DT, Slatter T. Protocol for tool wear measurement in micro-milling. *Wear.* 2019; 420-421:54-67.
- [8] Tansel I, Nedbouyan A, Tryillo M, Tansel B. Micro-end-milling-ii - Extending tool life with a smart workpiece holder (swh). *Int. J. Mach. Tools Manuf.* 1998; 38:1437-1448.
- [9] Karpat Y, Oliaei SNB. Influence of tool wear on machining forces and tool deflections during micro milling. *Int. J. Adv. Manuf. Technol.* 2016; 84:1963-1980.
- [10] Filiz S, Conley CM, Wasserman, MB, Ozdoganlar OB. An experimental investigation of micro-machinability of copper 101 using tungsten carbide micro-endmills. *Int. J. Mach. Tools Manuf.* 2007; 47:1088-1100.
- [11] Kim CJ, Bono M, Ni J. experimental analysis of chip formation in micro-milling. *Tech. Pap. Soc. Manuf. Eng. Ser.* 2002.
- [12] Aurich JC, Bohley M, Reichenbach IG, Kirsch B. Surface quality in micro milling: Influence of spindle and cutting parameters. *CIRP Annals – Man. Tech.* 2017; 66:101-104.
- [13] Tamborlin MO, Mewis J, Wasnievski L, Ramos SL, Schützer K. Influence of cutting parameters in micro-milling of moulds for micro-components. 16th Int. Sc. Conf. Prod. Eng. 2017, June 8-10 (Zagreb).
- [14] Rahman M, Kumar AS, Prakash JRS. Micro milling of pure copper. *J. Mat. Proc. Tech.* 2001; 116:36-43.